Decentralized Model Predictive-Based Load-Frequency Control in an Interconnected Power System Concerning Wind Turbines

T.H. Mohamed, J. Morel, H. Bevrani, A.A Hassan, Y. S Mohamed, T. Hiyama

Published (to be published) in: ***IEEJ TRANSACTIONS ON ELECTRICAL AND ELECTRONIC ENGINEERING***

(Expected) publication date: **2012**

Citation format for published version:

T.H. Mohamed, J. Morel, H. Bevrani, A.A Hassan, Y. S Mohamed, T. Hiyama (2012) Decentralized model predictive-based load-frequency control in an interconnected power system concerning wind turbines. IEEJ Transactions on Electrical and Electronic Engineering, vol. 7, pp. 487-494, June 2012, DOI: 10.1002/tee.21762

IEEJ TRANSACTIONS ON ELECTRICAL AND ELECTRONIC ENGINEERING
IEEJ Trans 2012; **7**: 487–494
Published online in Wiley Online Library (wileyonlinelibrary.com). DOI:10.1002/tee.21762

Paper

Decentralized Model Predictive-Based Load-Frequency Control in an Interconnected Power System Concerning Wind Turbines

Tarek Hassan Mohamed*[a], Non-member
Jorge Morel**, Non-member
Hassan Bevrani***, Non-member
Ahmed Abd-Eltawwab Hassan****, Non-member
Yehia Sayed Mohamed****, Non-member
Takashi Hiyama**, Member

This paper presents a load-frequency control (LFC) design using the model predictive control (MPC) technique in a multi-area power system in the presence of wind turbines (WTs). In the studied system, the controller of each local area is designed independently such that the stability of the overall closed-loop system is guaranteed. A frequency response model of the multi-area power system including WTs is introduced, and physical constraints of the governors and turbines are considered. The model was employed in the MPC structures. Digital simulations for a two-area power system are provided to validate the effectiveness of the proposed scheme. The results show that with the proposed MPC technique the overall closed-loop system performance shows robustness in the face of uncertainties due to governor and turbine parameter variation and load disturbances. A performance comparison between the proposed controller with WTs and MPC without WTs and a classical integral control scheme is carried out, confirming the superiority of the proposed MPC technique with WTs. © 2012 Institute of Electrical Engineers of Japan. Published by John Wiley & Sons, Inc.

Keywords: load-frequency control, integral control, wind turbine, model predictive control, decentralized control

Received 28 March 2011; Revised 16 June 2011

1. Introduction

In a load-frequency control (LFC) problem, area load change and abnormal conditions lead to mismatches in frequency and scheduled power interchanges between areas. These mismatches have to be corrected by the LFC system. LFC objectives, i.e. frequency regulation and tracking the load demands, maintaining the tie-line power interchanges to specified values in the presence of modeling uncertainties, system nonlinearities and area load disturbances, determine the LFC synthesis as a multiobjective optimization problem [1,2].

The fixed parameters controller, like an integral controller or a proportional integral (PI) controller, is widely employed in LFC application. Fixed parameters controllers are designed at nominal operating points and may not be suitable in all operating conditions. For this reason, adaptive gain scheduling approaches have been proposed for LFC synthesis [3,4]; this method is able to avoid the disadvantages of the conventional proportional integral differential PID controller, such as the need of adaptation of controller parameters, but actually it faces some difficulties, such as the instability of transient response (as a result of abruptness in the system parameters) and impossibility of obtaining accurate linear time-invariant models at variable operating points [3].

Recently, the model predictive control (MPC) has been shown to be an efficient strategy in many control applications in industry; it has many advantages such as very fast response and robustness against load disturbance and parameter uncertainty. Its straightforward design procedure is considered a major advantage of the MPC. Given a model of the system, only an objective function incorporating the control objectives needs to be set up. Additional physical constraints can be easily dealt with by adding them as inequality constraints, whereas soft constraints can be accounted for in the objective function using large penalties. Moreover, MPC adapts well to different physical setups and allows for a unified approach [5,6].

Recently, some papers have reported the application of MPC technique on the LFC issue [7–9]. In Ref. [7], fast response and robustness against parameter uncertainties and load changes can be obtained using the MPC controller, but only for single-area LFC application. In Ref. [8], the usage of MPC in multi-area power system was discussed, but only from the economy viewpoint; it presented a new model predictive LFC including economy logic for LFC cost reduction. In Ref. [9], feasible cooperation-based MPC is used in distributed LFC instead of centralized MPC which is impractical for the control of large-scale systems, such as power systems, In spite of the good effort made in Ref. [9], the authors did not deal with the problem of system's parameter mismatch, and they only discussed the effect of load change; in addition, the range of load change used in the case study was very large and inappropriate in the LFC issue.

In Ref. [10], the impacts of parametric uncertainties, besides the load change effect, in an interconnected power system with decentralized model predictive based LFC were discussed, and

[a] Correspondence to: Tarek Hassan Mohamed.
E-mail: tarekhie@yahoo.com

* High Institute of Energy, Aswan University, 1-sahary, Aswan, Egypt
** Department of Electrical Engineering & Computer Science, Kumamoto University, 2-39-1, Kurokami, Kumamoto 860-0864, Japan
*** Department of Electrical Engineering & Computer Science, University of Kurdistan, Kurdistan Region, Iran
**** Department of Electrical Engineering, Faculty of Engineering, Minia University, Cairo-Aswan road, Minia 61517, Egypt

results assured the ability of MPC to face the problem of large system parameter variation. Still the door is open to more efforts to enhance the system performance.

Variable speed wind turbines (VSWTs) are the most utilized type of modern wind turbines (WTs). They are partially or totally decoupled from the power network due to the power electronic converters which limits their capacity to provide primary frequency support to the network in case of disturbances. The inertial response of WTs is discussed in detail, e.g. in Refs [11,12]. In Ref. [11], a detailed background of frequency responses, including primary and secondary responses, is given. A detailed comparison between fixed-speed wind turbines (FSWTs) and doubly fed induction generator (DFIG) type WTs was made through detailed simulations. The potential of FSWTs to contribute to the frequency response has been shown. Also, the contribution DFIG-based WTs has been illustrated. In [12], it is reported that full converter type WTs are completely decoupled from the power grid and no contribution is given to the frequency regulation. On the other hand, it is pointed out that the DFIG-type WTs have some small contribution to the power network.

This paper studies the effect of merging the WTs in the system used in [10] on the system frequency response.

In this paper, each local area includes an aggregated WT model (which consists of 200 WT units) beside the main generation unit. The controller of each area can be designed independently. The MPC technique law produces its optimal output derived from a quadratic cost function minimization based on the dynamic model of the specified area. The technique calculates the optimal control signal while respecting the given constraints over the output frequency deviation and the load change. The effects of the physical constraints such as generation rate constraint (GRC) and speed governor dead band [1] are considered. The power system with the proposed MPC technique has been tested through the effect of uncertainties due to governor and turbine parameter variation and load disturbances using computer simulation. A comparison has been made between the proposed system (with MPC controller and participation of WT) and that system (with MPC controller but without WT participation) and the traditional one (system without WT participation and with conventional integral controller), confirming the superiority of the proposed system with WT. The simulation results prove that the proposed controller guarantees robust performance in the presence of uncertainties due to governor and turbine parameter variations and loads disturbances.

The rest of the paper is organized as follows: The description of the dynamics of the interconnected power system is given in Section 2. A general consideration about MPC and its cost function are presented in Section 3. In Section 4, a simplified WT model for frequency studies is presented. The proposed methodology is applied to two- and three-area power systems as cases studies in Section 5. Finally, the paper is concluded in Section 6.

2. System Dynamics

A multi-area power system comprises areas that are interconnected by tie-lines. The trend of the frequency measured in each control area is an indicator of the trend of the mismatch of power in the interconnection and not in the control area alone. The LFC system in each control area of an interconnected (multi-area) power system should control the interchange power with the other control areas as well as its local frequency. Therefore, the dynamic LFC system model must take into account the tie-line power signal. For this purpose, consider Fig. 1, which shows a power system with N-control areas [1]. In this section, a frequency response model for any area i of N power system control areas with an aggregated generator unit in each area is described [1].

The overall generator–load dynamic relationship between the incremental mismatch power ($\Delta \boldsymbol{P}_{mi} - \Delta \boldsymbol{P}_{Li}$) and the frequency

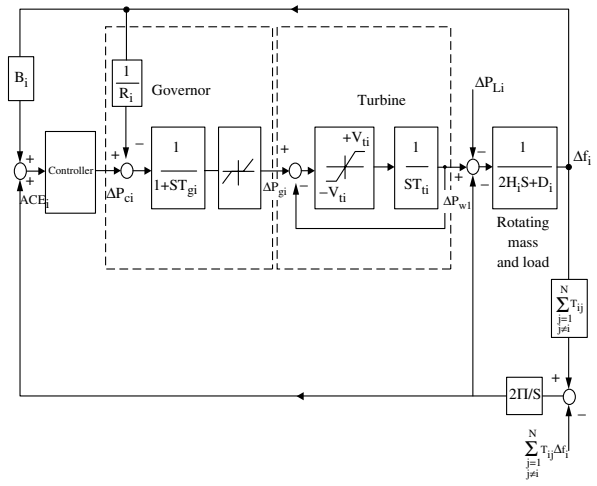

Fig. 1. Dynamic model of a control area in an interconnected environment

deviation ($\Delta \boldsymbol{f}_i$) can be presented as

$$\Delta \mathbf{f}_i = \left(\frac{1}{2H_i}\right).\Delta \boldsymbol{P}_{mi} - \left(\frac{1}{2H_i}\right).\Delta \boldsymbol{P}_{Li} - \left(\frac{D_i}{2H_i}\right).\Delta \boldsymbol{f}_i - \left(\frac{1}{2H_i}\right).\Delta \boldsymbol{P}_{tie,i} \quad (1)$$

where dynamics of the governor can be expressed as

$$\Delta \boldsymbol{P}_{mi} = \left(\frac{1}{\mathbf{T}_{ti}}\right).\Delta \boldsymbol{P}_g \quad (2)$$

The dynamics of the turbine can be expressed as

$$\Delta \boldsymbol{P}_{gi} = \left(\frac{1}{\boldsymbol{T}_{gi}}\right).\Delta \boldsymbol{P}_{ci} - \left(\frac{1}{\boldsymbol{R}_i \boldsymbol{T}_{gi}}\right).\Delta f_i - \left(\frac{1}{\boldsymbol{T}_{gi}}\right).\Delta \boldsymbol{P}_{gi} \quad (3)$$

the total tie-line power change between area $\boldsymbol{i}$ and the other areas can be calculated as

$$\Delta \boldsymbol{P}_{tie,i} = 2\pi.\left[\sum_{\substack{j=1 \\ j\neq i}}^{N} \boldsymbol{T}_{ij}\,\Delta \boldsymbol{f}_i - \sum_{\substack{j=1 \\ j\neq i}}^{N} \boldsymbol{T}_{ij}\,\Delta \boldsymbol{f}_j\right] \quad (4)$$

In a multi-area power system, in addition to regulating the area frequency, the supplementary control should maintain the net interchange power with neighboring areas at predetermined values. This is generally accomplished by adding a tie-line flow deviation to the frequency deviation in the supplementary feedback loop. A suitable linear combination of frequency and tie-line power changes for area i is known as the area control error (ACE), given by

$$\boldsymbol{ACE}_i = \Delta \boldsymbol{P}_{tie,i} + \boldsymbol{B}_i\,\Delta \boldsymbol{f}_i \quad (5)$$

Equations (1)–(4) represent the frequency response model for N power system control areas with one generator unit in each area and can be combined in the following state space model:

$$\left\{\begin{array}{c} \begin{bmatrix} \Delta P_{gi} \\ \Delta P_{mi} \\ \Delta f_i \\ \Delta P_{tie,i} \end{bmatrix} = \begin{bmatrix} -\frac{1}{T_{gi}} & 0 & -\frac{1}{R_i T_{gi}} & 0 \\ \frac{1}{T_{ti}} & -\frac{1}{T_{ti}} & 0 & 0 \\ 0 & \frac{1}{2H_i} & -\frac{D_i}{2H_i} & -\frac{1}{2H_i} \\ 0 & 0 & \sum_{\substack{j=1 \\ j\neq i}}^{N} T_{ij} & 0 \end{bmatrix} \begin{bmatrix} \Delta P_{gi} \\ \Delta P_{mi} \\ \Delta f_i \\ \Delta P_{tie,i} \end{bmatrix} \\ + \begin{bmatrix} 0 & 0 \\ 0 & 0 \\ \frac{1}{2H_i} & 0 \\ 0 & -2\pi \end{bmatrix} \begin{bmatrix} \Delta P_{Li} \\ \Delta v_i \end{bmatrix} + \begin{bmatrix} \frac{1}{T_{gi}} \\ 0 \\ 0 \end{bmatrix} \Delta P_{ci} \\ y = ACE_i = [0 \quad 0 \quad B_i \quad 1] \end{array}\right\} \quad (6)$$

where
ΔP_{gi} : the governor output change of area i;
ΔP_{mi} : the mechanical power change of area i;
Δf_i : the frequency deviation of area i;
ΔP_{Li} : the load change of area i;
ΔP_{ci} : supplementary control action of area i;
y_i : the system output of area i;
H_i : equivalent inertia constant of area i;
D_i : equivalent damping coefficient of area i;
R_i: speed drop characteristic of area i;
T_{gi}, T_{ti}: governor and turbine time constants of area i;
ACE_i : the control error of area i;
B_i: frequency bias factor of area i;
T_{ij}: tie-line synchronizing coefficient with area j;
$\Delta P_{\text{tie},i}$: the total tie-line power change between area i and the other areas;
Δv_i : control area interface, $\Delta v_i = \sum_{\substack{j=1 \\ j\neq i}}^{N} \boldsymbol{T}_{ij} \Delta \boldsymbol{f}_j$

3. Model Predictive Control

The MPC has been proven to efficiently control a wide range of applications in industry such as chemical process, petroleum industry, electromechanical systems, and many others. The MPC scheme is based on an explicit use of a prediction model of the system response to obtain the control actions by minimizing an objective function. The effectiveness of the MPC is demonstrated to be equivalent to optimal control. Its main strengths lie in its computational expediency, real-time applications, intrinsic compensation for time delays, treatment of constraints, and potential for future extensions of the methodology. At each control interval, the first input in the optimal sequence is sent into the plant, and the entire calculation is repeated at subsequent control intervals. The purpose of taking new measurements at each time step is to compensate for unmeasured disturbances and model inaccuracy, both of which cause the system output to be different from the one predicted by the model [5,6].

Figure 2 shows a simple structure of the MPC controller. An internal model is used to predict the future plant outputs based on the past and current values of the inputs and outputs and on the proposed optimal future control actions. The prediction has two main components: the free response which is the expected behavior of the output assuming zero future control actions, and the forced response which is the additional component of the output response due to the candidate set of future controls. For a linear system, the total prediction can be calculated by summing both of free and forced responses; the reference trajectory signal is the target value the output should attain. The optimizer is used to calculate the best set of future control action by minimizing a cost function (J), and the optimization is subject to constraints on both the manipulated and controlled variables [13].

The general object is to tighten the future output error to zero with minimum input effort. To minimize the cost function, it is generally a weighted sum of squared predicted errors and square future control values, e.g. in the generalized predictive control (GPC):

$$J(N1, N2, Nu) = \sum_{j=N_1}^{N_2} \beta(j)[\hat{y}(k+j|k) - w(k+j)]^2 + \sum_{j=1}^{N_u} \lambda(j)[u(k+j-1)]^2 \quad (7)$$

where N_1, N_2 are the lower and upper prediction horizons over the output, N_u is the control horizon, and $\beta(j), \lambda(j)$ are weighting factors. The control horizon permits the decrease of the number of calculated future control according to the relation:

$$\Delta u(k+j) = 0 \text{ for } j \geq N_u$$

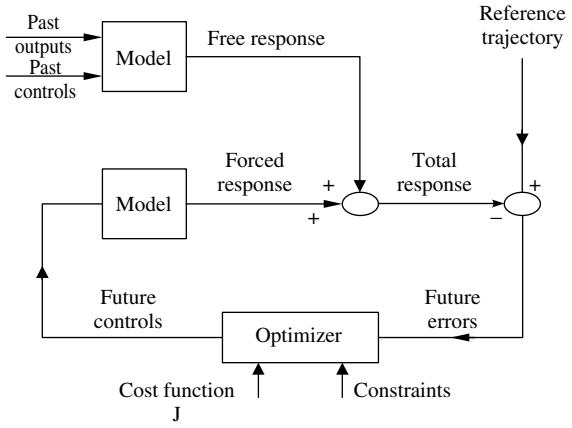

Fig. 2. A simple structure of the MPC controller

$w(k+j)$ represents the reference trajectory over the future horizon N.

Constraints over the control signal, the outputs, and the control signal change can be added to the cost function:

$$\begin{aligned} u_{\min} &\leq u(k) \leq u_{\max} \\ \Delta u_{\min} &\leq \Delta u(k) \leq \Delta u_{\max} \\ y_{\min} &\leq y(k) \leq y_{\max} \end{aligned} \quad (8)$$

Solution of (7) gives the optimal sequence of the control signal over the horizon N while respecting the given constraints of (8).

As the control horizon and the prediction horizon both approach infinity and when there are no constraints, we obtain the standard linear quadratic regulator problem, which was studied extensively in the 1960s and 1970s. The optimal control sequence is generated by a static state feedback law where the feedback gain matrix is found via the solution of an algebraic Riccati equation. This feedback law has some well-known nice properties; in particular, it guarantees closed-loop stability for any positive semidefinite weighting matrix **Q** and any positive definite **R**. With constraints, an infinite-dimensional optimization problem results, which is—at least at first sight—not a very practical proposition. On the other hand, by choosing both the control and the output horizons to be finite, the quadratic program is finite dimensional and can be solved relatively easily online at every time step [14].

The optimal control problems with state-space uncertainty descriptions through linear matrix inequalities are solved [15]. For the technique proposed in Ref. [16], where a worst case quadratic performance criterion is minimized over a finite set of models subject to input/state constraints, problems with more than 1000 variables and 5000 constraints can be solved in a few minutes on a workstation by using interior-point methods.

MPC has many advantages: in particular, it can pilot a big variety of processes; it is simple to apply in the case of multivariable system; it can compensate for the effect of pure delay by the prediction; it can induce the anticipated effect in closed loop; it is a simple control technique that can be applied; and it also offers optimal solution while respecting the given constraints.

On the other hand, this type of restructure requires the knowledge of the model of the system, and in the presence of constraints, it becomes a more complex regulator than the PID for example, and it takes more time for online calculations.

4. Simplified Wind Turbine Model for Frequency Studies

Figure 3 shows a simplified model of DFIG-based WT for frequency response; this model is investigated from the detailed model [17], which can be described as

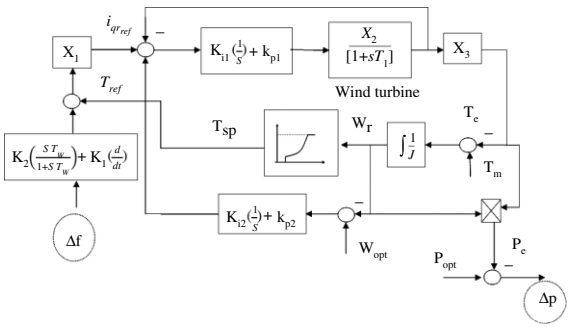

Fig. 3. Simplified model of DFIG-based WT

Voltage equations

$$V_{ds} = R_S i_{ds} - \psi_{qs} + \frac{1}{w_S}\frac{d}{dt}\psi_{ds} \tag{9}$$

$$V_{qs} = R_S i_{qs} - \psi_{ds} + \frac{1}{w_S}\frac{d}{dt}\psi_{qs} \tag{10}$$

$$V_{dr} = R_r i_{dr} - s\psi_{qs} + \frac{1}{w_S}\frac{d}{dt}\psi_{dr} \tag{11}$$

$$V_{qr} = R_r i_{qr} - \psi_{dr} + \frac{1}{w_S}\frac{d}{dt}\psi_{qr} \tag{12}$$

Flux equations

$$\psi_{ds} = L_{ss} i_{ds} + L_m i_{dr} \tag{13}$$

$$\psi_{qs} = L_{ss} i_{qs} + L_m i_{qr} \tag{14}$$

$$\psi_{dr} = L_{rr} i_{dr} + L_m i_{ds} \tag{15}$$

$$\psi_{qr} = L_{rr} i_{qr} + L_m i_{qs} \tag{16}$$

where $L_{ss} = L_s + L_m$ and $L_{rr} = L_r + L_m$
Torque equation

$$T_e = \psi_{ds}.i_{qs} - \psi_{qs}.i_{ds} = \psi_{dr}.i_{qr} - \psi_{qr}.i_{dr} \tag{17}$$

By manipulating (9)–(13), the following equations can be derived:

$$i_{dr} = -\frac{w_S R_r}{L_{rr}} i_{dr} + s.w_s.i_{qr} + \frac{w_s}{L_{rr}} v_{dr} + s.w_s.\frac{L_m}{L_{rr}}.i_{qs} - \frac{L_m}{L_{rr}}.i_{ds} \tag{18}$$

$$i_{qr} = -\frac{w_S R_r}{L_{rr}} i_{qr} + s.w_s.i_{dr} + \frac{w_s}{L_{rr}} v_{qr} + s.w_s.\frac{L_m}{L_{rr}}.i_{ds} - \frac{L_m}{L_{rr}}.i_{qs} \tag{19}$$

As shown in Fig. 3, the inertia response of the DFIG is obtained by adding a supplementary control loop to the torque control loop of the DFIG wind turbine. When a frequency event occurs, the supplementary loop acts on $i_q s_{ref}$ and changes vqr. Therefore, it was assumed that when a DFIG provides primary response, there is no change in i_{dr} or i_{ds}.

For vector control of the DFIG, the d-axis was chosen such that it coincided with the maximum of the stator flux; therefore $\psi_{ds} = 1$ pu and $\psi_{qs} = 0$ pu. Substituting in (14), the following equation can be obtained:

$$i_{qs} = -\frac{L_m}{L_{ss}} i_{qr} \tag{20}$$

Then (11) can be simplified and converted to the S-domain as

$$S\left[1 - \frac{L_m^2}{L_{ss}L_{rr}}\right] i_{qr} = \frac{w_s R_r}{L_{rr}} i_{qr} + \frac{w_s}{L_{rr}} v_{dr} \tag{21}$$

and

$$i_{qr} = \frac{1}{R_r}.\frac{1}{[1+ST_1]} v_{qr} \tag{22}$$

substituting $\psi_{ds} = 1$ pu and $\psi_{qs} = 0$ pu in (17) and the using (20), the following equation can be obtained for the electromagnetic torque:

$$T_e = i_{qs} = -\frac{L_m}{L_{ss}} i_{qr} \tag{23}$$

A supplementary speed control loop has been added to enhance the turbine performance. As shown in the Fig. 3, the frequency deviation is applied to the supplementary control loop to give that control signal which is added to torque set point T_{sp} to give the reference torque signal T_{ref}; the reference torque signal is multiplied by the gain X_1 to give the current reference command signal $i_{qr_{ref}}$; and this current reference command signal is added to the output of the supplementary speed control loop and the negative feedback current signal i_{qr} to give a current error signal which is fed to the PI control signal to give voltage command v_{qr}. This voltage command v_{qr} is fed to the WT dynamic block to give the actual current signal i_{qr} which is multiplied by the gain X_3 to give the electromagnetic torque T_e which is subtracted from the mechanical torque signal and multiplied by WT inertia to give the rotational speed of the WT w_r.

In this paper, the WT will be considered as a supplementary LFC part, so the WT dynamic will not be included in the MPC state space model. Table I shows the detailed expressions of the main parameters utilized for the simplified model of Fig. 3.
where

$$L_0 = \left[L_{rr} + \frac{L_m^2}{L_{ss}}\right]$$

$$L_{ss} = L_s + L_m$$

$$L_{rr} = L_{rs} + L_m$$

L_m: the magnetizing inductance.
R_r and R_s: the rotor and stator resistances, respectively.
L_r and L_s: the rotor and stator leakage inductances, respectively.
L_{rr} and L_{ss}: the rotor and stator self-inductances, respectively.
w_s: synchronous speed.

5. Results and Discussion

Computer simulations have been carried out in order to validate the effectiveness of the proposed scheme. The Matlab/Simulink software package has been used for this purpose.

The simulation studies were carried out for the proposed controllers with GRC of 10% per minute, and the maximum value of dead band for governor was specified as 0.05 pu for each area [1]. The parameters of the MPCi controller of area i were set as follows:
Prediction horizon = 13,
Control horizon = 2,
Weights on manipulated variables = 0,
Weights on manipulated variable rates = 0.1,
Weights on the output signals = 1, (all weights and horizon values are determined using try and error method.)
Sampling interval = 0.0002 s.
Constraints are imposed over the control action, and frequency deviation are considered as follows:
Maximum control action = 0.25 pu.
Minimum control action = −0.25 pu.
Maximum frequency deviation = 1 pu.

Table I. Parameters for Fig. 3

X_1	X_2	X_3	T_1
$\frac{-L_{ss}}{L_m}$	$\frac{1}{R_r}$	$\frac{L_m}{L_{ss}}$	$\frac{L_0}{w_S R_s}$

Table II. WT parameters and operating point

1Operating point (MW)	247
Wind speed (m/s)	11
Rotational speed (pu)	1.17
R_r(pu)	0.00552
R_s(pu)	0.00491
X_{lr}(pu)	0.1
X_{ls}(pu)	0.09273
X_m(pu)	3.9654
H_t(pu)	4.5

X_{m} is the magnetizing reactance, $(P_{wt})_{\mathrm{Base}} = 400$ MVA, and $(w_r)_{\mathrm{base}} = 1.15$ rad s.

Minimum frequency deviation $= -1$ pu.

The WT used consists of 200 units of 2 MW rated VSWTs; the WT parameters and operating point are indicated in Table II.

The parameters of the used in WT model are as follows:
$K_1 = 0.00125$, $K_2 = 0.02$, and $T_w = 1$ s,
$K_{p1} = 10$, $K_{i1} = 10$,
$K_{p2} = 0.8$, $K_{i2} = 4$.

5.1. Scenario A In this scenario, a two-control area power system, shown in Fig. 4 is considered as a test system to illustrate effectiveness of the proposed control strategy. Each area consists of a synchronous generator (with a rated power of 800 MW), the overall rotating mass and load, and an aggregated generator unit including one nonlinear turbine with GRC and one governor with dead-band constraint [1].

The controller of each area can be designed independently according to the linear state-space model described in (6). On the other hand, the frequency deviation is used as a feedback for the closed-loop control system. The measured and reference area control error $ACEi$, ($\mathrm{ACE}_{\mathrm{ref}} = 0$ Hz) are fed to the MPC in order to obtain the supplementary control action ΔP_{ci} which is added to the negative frequency feedback signal.

The resulting signal is fed to the governor giving the governor valve position which supplies the turbine to give the mechanical power change ΔP_{mi} which is affected by the load change ΔP_{Li} and the tie-line power change $\Delta P_{tie,i}$ giving the input of the rotating mass and load block to provide the actual frequency deviation Δf_i. In addition, the tie-line flow deviation is added to the frequency deviation in the supplementary feedback loop to give the area control error ACE_i. Also, each area has its own aggregated WT model (which consists of 200 WT units of 2 MW rated VSWTs [18]) which is fed by the frequency deviation and produces its electrical power deviation which is multiplied by a gain equal to 0.5 (to make a correlation between power system and WT bases), and used to adjust the total power change ΔP_{mi} as shown in the figure. The used practical two-area power system had the nominal parameters [1] listed in Table III.

5.1.1. Case 1 In this case, the system performance with the proposed MPC controllers in case of WT participation at nominal parameters was tested and compared with the system performances with both MPC controllers without WT participation and using a conventional integrator in the presence of load change in area 2. Figure 5 shows the simulation results in this case. The results from the top to the bottom are: the frequency deviations of area 1 (Δf_1), the frequency deviations of area 2 (Δf_2), and the tie-line power change between area 1 and area 2 ($\Delta P_{tie,1}$) using the proposed MPC with and without WTs, and using conventional integrator controllers following a step load change in area 2 (ΔP_{L2} is assumed to be 0.02 pu at $t = 30$ s). It is noteworthy that with the proposed MPC controller with WT, the system is more stable and fast comparing with other two controllers.

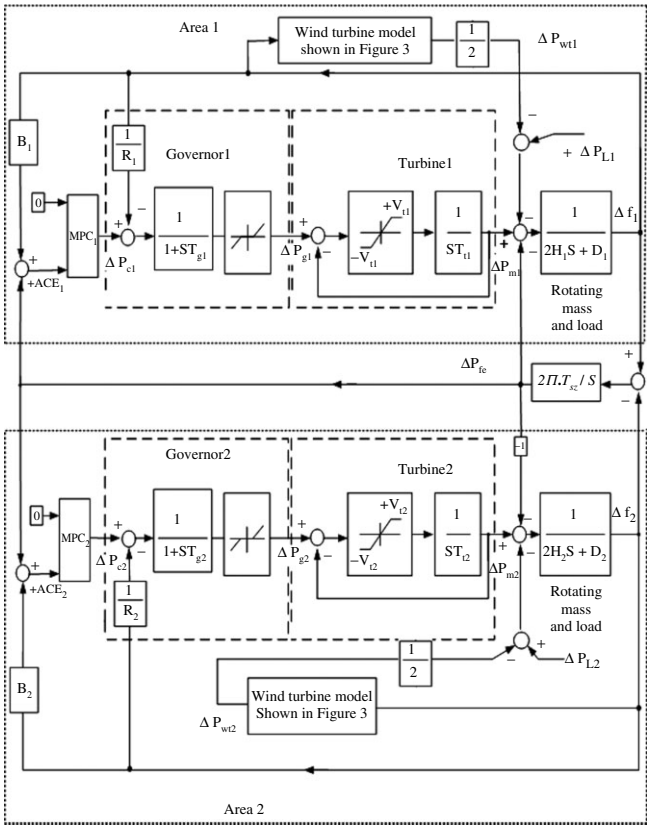

Fig. 4. The block diagram of two area power system including the proposed MPC controllers

Table III. Parameters and data of a practical two-area power system.

Parameter	Area 1	Area 2
K(s)	-0.3/s	-0.2/s
D(pu/Hz)	0.015	0.016
$2H$(pu.s)	0.1667	0.2017
R(Hz/pu)	3.00	2.73
$T_g(s)$	0.08	0.06
$T_t(s)$	0.40	0.44
T_{12}	0.20	

$(P_e)_{\mathrm{Base}} = 800$ MVA.

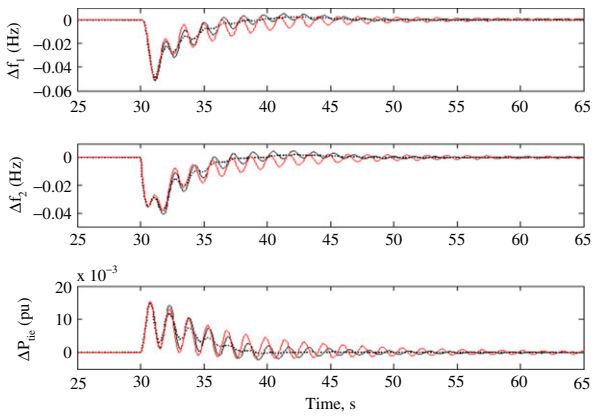

Fig. 5. Power system response to case 1 with (MPC + WT) (solid and bold), with (MPC only)(dotted), and with conventional controller (solid)

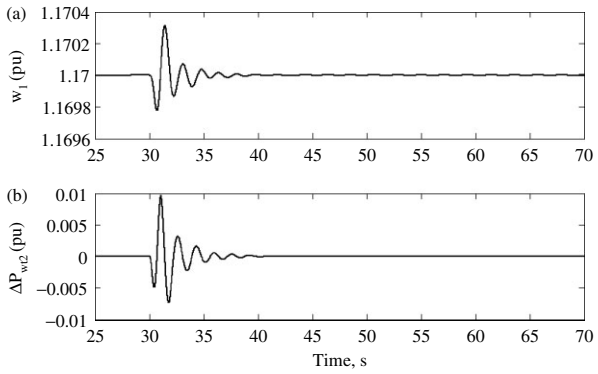

Fig. 6. Area 1 WT responses to case 1

Figure 6 shows both the rotational speed (at the top) and power change of WT in area 1 (at the bottom). As shown in this figure, a small change in the WT electrical power can cooperate in enhancement of the total system response.

5.1.2. Case 2 In this case, the robustness of the proposed MPC controller in presence of WT has been tested at a severe case of parameter uncertainty. In this case, the governor and turbine time constants of the two areas were increased to $T_{g1} = 0.105$ s (≅31% change), $T_{t1} = 0.785$ s (≅95% change), $T_{g2} = 0.105$ s (≅66% change) and $T_{t2} = 0.6$ s (≅38% change), respectively (this can happen if both turbine and governor are replaced by a new parts, for maintenance purposes etc., and the MPC controller keeps the values of the old parts). Figure 7 depicts the response of the MPC controllers in the presence of above uncertainty, under at same load change described in the first case. The results from the top to the bottom are: frequency deviation in area 1, frequency deviation in area 2, and tie-line power change. It is seen that a desirable performance response has been achieved using the MPC controller. This is because the MPC provides feedback compensation for the model uncertainty. In contrast, with a conventional integrator, the performance and stability are seriously degraded. Also, the figure indicates that the presence of WT leads to enhancement of the system performance with the MPC controller significantly.

5.2. Scenario B To illustrate the behavior of LFC system with the proposed decentralized MPC controller in the presence of WT in a multi-area power system, consider three identical interconnected control areas as shown in Fig. 8. The simulation parameters [1] are given in Table IV, while the WT parameters

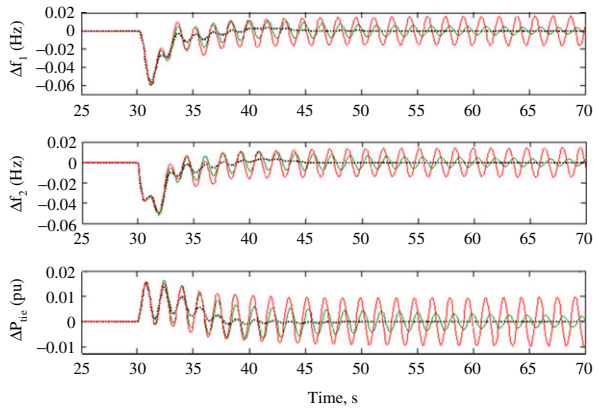

Fig. 7. Power system response to case 2 with (MPC + WT) (solid and bold), with (MPC only)(dotted), and with conventional controller (solid)

Table IV. Parameters and data of a practical three control area power system

Parameter	Area 1	Area 2	Area 3
K(s)	−0.3/s	−0.2/s	−0.4/s
D(pu/Hz)	0.015	0.016	0.015
$2H$(pu.s)	0.1667	0.2017	0.1247
R(Hz/pu)	3.00	2.73	2.82
$T_g(s)$	0.08	0.06	0.07
$T_t(s)$	0.40	0.44	0.3
T_{ij}	$T_{12} = 0.20$ $T_{13} = 0.25$	$T_{21} = 0.20$ $T_{23} = 0.15$	$T_{31} = 0.25$ $T_{32} = 0.15$

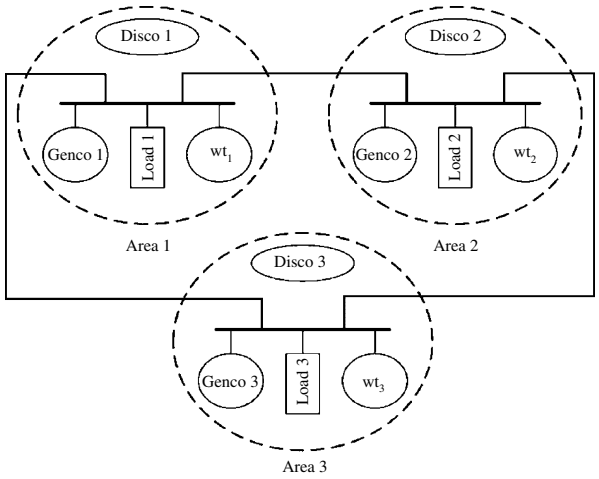

Fig. 8. Three-control area power system with WTs

are as listed in Table III. To investigate the robustness of the proposed system in case of system parameter uncertainties, the system is tested at a simultaneous 0.02-pu load step disturbance in control area 2 and against wide range of parameter uncertainty is validated. In this case, the governor and turbine time constants of each area is increased to $T_{g1} = 0.105$ s (≅31% change), $T_{t1} = 0.785$ s (≅95% change), $T_{g2} = 0.105$ s (≅66% change) and $T_{t2} = 0.6$ s (≅38% change), $T_{g3} = 0.15$ s (≅100% change) and $T_{t3} = 0.7$ s (≅100% change), respectively. Figure 9 depicts the response of the proposed MPC controllers in the presence of WT, without WT, and classical integrator controller in the case of above uncertainty. The results from the top to the bottom are: frequency deviation

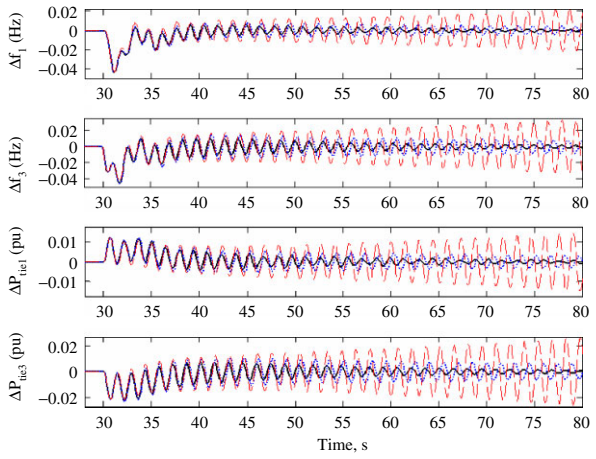

Fig. 9. Power system responses to scenario B with (MPC + WT) (solid and bold), only MPC controller (dotted), and conventional controller (solid)

in area 1, frequency deviation in area 3, tie-line power change in area 1, and tie-line power change in area 3. This figure shows that even at this severe condition of uncertainties, the system with MPC controllers keeps stable, while it becomes unstable with integrator controllers. And it appears that WT affects positively on the system response.

6. Conclusion

This paper presented the merging of WTs in an interconnected power system controlled by a robust LFC based on the MPC technique. The proposed method was applied to a two- and three-control-area power system with parametric uncertainty and various loads conditions. Digital simulations were carried out to validate the effectiveness of the proposed scheme. The proposed controller was tested for several mismatched parameters and load disturbances.

A performance comparison between the proposed MPC in the presence of WT and MPC without WT and conventional integrator controllers was carried out. The simulation results demonstrated that the closed-loop system with MPC controller was robust against the parameter perturbation of the system and had desirable performance in comparison with the classical integral control design in all performed test scenarios. Also, it was noted that the WT had a positive effect on the total response of the system.

References

(1) Bevrani H. *Robust Power System Frequency Control.* Springer: New York; 2009.
(2) Bevrani H, Hiyama T. On-line load-frequency regulation with time delays: Design and real-time implementation. *IEEE Transactions on Energy Conversion* 2009; **24**(**1**):292–300.
(3) Chang CS, Fu W. Area load frequency control using fuzzy gain scheduling of PI controllers. *Electric Power Systems Research* 1997; **42**(**1**):145–152.
(4) Talaq Al-Basri F. Adaptive fuzzy gain scheduling for load frequency control. *IEEE Transactions on Power Systems* 1999; **14**(**1**):145–150.
(5) Thomas J, Dumur D, Buisson J, Gueguen H. Model predictive control for hybrid systems under a state partition based MLD approach (SPMLD). *International Conference on Informatics in Control, Automation and Robotics ICINCO'04*, Setúbal 2004; **3**:78–85.
(6) Richalet J, Rault A, Testud JL, Japon J. "Model predictive heuristic control", application to industrial processes. *Automatica* 1978; **14**(**5**):413–428.
(7) Mohamed TH, Bevrani H, Hassan AA, Hiyama T. Model Predictive Based Load Frequency Control Design. *16th International Conference of Electrical Engineering*, July 2010, Busan, Korea.
(8) Rerkpreedapong D, Atic N, Feliachi A. Economy oriented model predictive load frequency control. *Power Engineering, 2003 Large Engineering Systems Conference on Volume*, 2003; 12–16.
(9) Venkat AN, Hiskens IA, Rawlings JB, Wright SJ Distributed MPC strategies with application to power system automatic generation control. *IEEE Transactions on Control Systems Technology* 2008; **16**(**6**):1192–1206.
(10) Mohamed TH, Bevrani H, Hassan AA, Hiyama T. Decentralized model predictive based load frequency control in an interconnected power system. *Energy Conversion and Management* 2011; **52**:1208–121.
(11) Mullane A, O'Malley M. The inertial response of induction-machine-based wind turbines. *IEEE Transactions on Power Systems* 2005; **20**(**3**):1496–1503.
(12) Holdsworth L, Ekanayake JB, Jenkins N. Power system frequency response from fixed speed and doubly fed induction generator-based wind turbines. *Wind Energy* 2004; **7**:21–35.
(13) De Silva CW. *Mechatronic Systems: Devices, Design, Control, Operation and Monitoring.* Taylor and Francis/CRC Press: Boca Raton, FL; 2007.
(14) Morari a M, Lee JH. Model predictive control: past, present and future. *Computers and Chemical Engineering* 1999; **23**:667–682.
(15) Kothare MV, Balakrishnan V, Morari M. Robust constrained model predictive control using linear matrix inequalities. *Automatica* 1996; **32**(**10**):1361–1379.
(16) Hansson A, Boyd S. Robust optimal control of linear discrete time systems using primal-dual interior-point methods. *Proceedings of American Control Conference* 1998; **1**:183–187.
(17) Ekanayake JB, Jenkins N, Strbac G. Frequency response from wind turbines. *Wind Engineering* 2008; **32**(**6**):573–586.
(18) Morel J, Bevrani H, Ishii T, Hiyama T. A robust control approach for primary frequency regulation through variable speed wind turbines. *IEEJ Transactions on Power and Energy* 2010; **130**(**11**): 1002–1009.

Tarek H. Mohamed (Non-member) was born in Libya in January 1975. He received the B.Sc. degree in automatic control from the Faculty of Electronics, Minofia, Egypt, in 1997, and M.Sc. degree from the Faculty of Engineering, Minia University, Egypt, in 2006, He is currently a Ph.D. exchange student at Kumamoto University, Japan. He is a member of the High institute of Energy, South Valley University, Egypt.

Jorge Morel (Non-Member) received the B.E. degree in electromechanical engineering from the National University of Asuncion, Paraguay, in 2000, and the M. Eng. and Ph.D. degrees in electrical engineering from Kumamoto University, Japan, in 2008 and 2011, respectively. Currently he is pursuing the Ph.D. degree in the Department of Computer Science and Electrical Engineering, Kumamoto University, Japan. His research interests include wind turbines and the application of intelligent and robust control techniques to power systems concerning wind generation.

Hassan Bevranni (Non-member) received the B.E. (Hons.) degree from K.N. Toosi University of Technology, Tehran, Iran, in 997, and the Ph.D. degree from Osaka University, Osaka, Japan, in 2004, both in electrical engineering. He is currently an Associate Professor with the Department of Electrical Engineering & Computer Science, University of Kurdistan, Iran. His current research interests include robust load-frequency control and robust/intelligent control applications in power system and power electronic industry.

Ahmed A. Hassan (Non-member) was born on November 12, 1954. He received the B.Sc. and M.Sc., degrees from Assuit University, Egypt, and the Ph.D. degree from EL-Minia University, Egypt, all in electrical engineering, in 1976, 1982, and 1988 respectively. Since 2001, he has been a Professor with the Electrical Engineering Department, EL-Minia University. He is currently also the Dean of the faculty of Computer Science and Information. His current interests include the application of advanced control techniques to electrical machine drives.

Yehia S. Mohamed (Non-member) was born in Assiut, Egypt, in January 1965. He received the B.S., M.Sc., and Ph.D. degrees, all in electrical engineering, from Faculty of Engineering, Minia University, Egypt, in 1987, 1992, and 1996, respectively. He is currently a member of the Faculty of Engineering, Minia University. His current research interests include the control of electrical machine drives.

Takashi Hiyama (Member) was born on March 14, 1947. He received the B.E, M.S., and Ph.D. degrees, all in electrical engineering, from Kyoto University, Japan, in 1969, 1971, and 1980, respectively. Since 1989, he has been a Professor with Department of Electrical and Computer Engineering, Kumamoto University, Japan. His current research interests include the application of intelligent system to power system operation, management, and control. Prof. Hiyama is a senior member of the IEEE and a member of the Japan Solar Energy Society.